5.1.1 AN ANALYSIS AT MESOSPHERIC COHERENT-SCATTER POWER ENHANCEMENTS DURING SOLAR FLARE EVENTS

J. Parker and S. A. Bowhill

Department of Electrical and Computer Engineering
University of Illinois
Urbana, IL 61801

ABSTRACT

Solar flares produce increases in coherent-scatter power from the mesosphere due to the increase in free electrons produced by X-ray photoionization. Thirteen such power enhancements have been observed at Urbana. When such an enhancement occurs at an altitude containing a turbulent layer with constant strength, we may estimate the relative enhancement of electron density from the enhancement in power. Such estimates of enhanced electron density are compared with estimates of the X-ray photoionization at that altitude, deduced from geostationary satellite measurements. It is found that possible types ion-chemical reaction scheme may be distinguished, and the nonflare ion-pair production function may be estimated. The type of ion-chemical scheme and the nonflare ion-production function are shown to depend on the solar zenith angle.

INTRODUCTION

It has, of course, been known for some time that solar flares produce an increase in ionization in the D region. This flare-time enhancement in ionization results in an increase in coherent scattered power which has been assumed to account for an exceptionally full set of good mesospheric velocity measurements during the event of April 11, 1978, 0800 CST at Urbana (MILLER et al., 1978), and also measured directly for the event of January 5, 1981, at 1218 AST at Arecibo (ROTTGER, 1983).

However, the processes linking the solar X-ray enhancement to the coherent-scatter power increase involve many unknowns. Photoionization by X-rays may be considered as the driving function of a set of ion-chemical reactions which finally determines the electron-density profile; this profile must then be advected by turbulence to produce the scattered power. Many details of these processes can only be deduced indirectly.

This paper describes how models of these processes may be constructed which account for some of the features of the power enhancements observed during solar flares. Early work along these lines may be found in PARKER and BOWHILL (1984).

COHERENT SCATTER DEPENDENCE ON ELECTRON DENSITY

The radar scattering cross section is proportioned to the mean-square fluctuation of the retractive index η. At VHF:

$$\eta^2 = 1 - Ne^2/\varepsilon_o m\omega^2$$

where N is the electron concentration, e and m the charge and mass of the electron, ε_o the permitivity of free space, and ω the angular frequency of the impinging wave. The right-hand term is small compared to unity, ε_o fluctuations in η and N are proportional. Further, if the electron concentration increases in a scattering volume by a constant factor, the mean-square fluctua-

tion in electron density ΔN^2 due to turbulence will be

$$\langle \Delta N^2 \rangle \propto (N')^2 \propto N^2$$

where N' is the vertical gradient of the electron density N. Thus, the scattered power P is proportional to N^2 within time-scales where the turbulence is characterized by constant mean-squared statistics. (This assumes no time-lag due to turbulent advection; we shall demonstrate below that this holds at least some of the time.

Finally, when we divide the flare-time scattered power P at a given altitude by the pre-flare power P_o we obtain

$$P/P_o = (N_o + \Delta N)^2/N_o^2$$

which implies

$$\Delta N/N_o = \sqrt{P/P_o} - 1$$

D-REGION FLARE EFFECTS OBSERVED AT URBANA

Table 1 displays features of 13 solar flare events which produced enhanced scatter, the enhancement shown for the altitude range 60-75 km. The sizes of the peak X-ray fluxes from two detectors on the GOES II satellite are shown for comparison. No correlation of X-ray event size and coherent-scatter power enhancement is evident. This is probably due to the wide variability of turbulent strength and the nonflare ion-production rate from one flare event to another. This suggests the need for a more sophisticated analysis.

MODELS RELATING SOLAR X-RAYS AND ELECTRON DENSITY

Given the GOES II X-ray measurements, we may calculate the X-ray ion-pair production rate q_x at a given altitude as follows. First, we must estimate the X-ray spectrum from the two data points provided by the GOES detectors at each time. This may be done by assuming a power law spectral form:

$$\Phi_\infty = A\lambda^B$$

(see for example ROWE et al., 1970) and solving for A and B based on the wavelength response characteristics of the X-ray detectors (published in DONNELLY, 1977).

This form of the X-ray intensity $\Phi_\infty(\lambda)$ is used to calculate the desired ion-pair production function q_x according to Chapman theory. Constants necessary for this calculation are the average air absorption cross sections $\sigma_a(\lambda)$ and the ionization efficiencies for X-rays $\eta(\lambda)$ from BANKS and KOCKERTS (1973), and the scale height H and average air density M from the US STANDARD ATMOSPHERE (1976).

The relationship between q (= $q_o + q_x$) and N is particularly unclear in the lower D region. If we assume overall charge neutrality, an unchanged ratio of negative ions and positive ions, and unchanged proportions of the recombining species, we may derive the following (MITRA, 1974):

$$q = \alpha N^2$$

where the constant of proportionality α is called the effective recombination coefficient (call this Case A). MITRA (1974) also proposes (Case B)

$$q = \beta N$$

Table 1. X-ray flare events producing measurable coherent-scatter radar power enhancements at Urbana between April 1978 and December 1983.

yr mo da cst	SID	Hα	pk flux x 10^{-5}w/m^2 0.1-0.8nm	0.05-0.4nm	61.5-75 km pk CS power dB above P_o
78 04 11 0820	3+	NA	20	3.5	7.7
80 05 21 1510	3	3B	14	3.2	29.8
80 05 28 1354	2+	2B	12	2.0	3.5
80 11 13 1324	2+	1N	4.2	0.7	11.2
80 11 14 1239	2+	1B	2.4	0.4	13.8
81 01 27 0947	2	1B	4.6	1.3	6.1
81 05 05 0809	3	3B	12	3.3	2.8
81 08 03 1425	2+	1N	7.1	1.8	10.1
81 10 14 1111	2+	1B	30	11	7.4
82 03 31 1626	2+	NA	7.5	1.7	4.9
82 06 02 0953	3+	NA	10	2.9	17.4
83 08 13 1215	1	2B	5.2	0.9	3.7
83 08 21 1159	1	2B	2.2	0.3	6.8

as a possible relationship, given other conditions. Both relationships require chemical equilibrium, which may or may not hold during a flare. If not, the relationship is far more complicated, but a model by THOMAS et al. (1973) predicts delays in the lower D region between peak q and peak N of up to 14 minutes, increasing with decreasing altitude (Case D).

DISTINGUISHING CHEMICAL SCHEME TYPES AND ESTIMATING NONFLARE ION-PAIR PRODUCTION

To distinguish between these three possibilities (and possibly others) at a given altitude we may assume each possiblity in turn, compare q_x at each time with $\Delta N/N0$ from the coherent-scatter data, and find the best fit. To simplify this comparison, note that Case A implies $P \propto q$, so that we may estimate q_x/q_o as

$$q_x/q_o = P/P_o - 1$$

For Case B, q and N are proportional, so that

$$q_x/q_o = \sqrt{P/P_o} - 1$$

If we make two plots, one for each of these estimates of q_x/q_o against the same values at q_x from the satellite data, the result would be a line of unit slope only for that case which is correct. If the points of the initial

part of the flare (ascending) do not lie along the same path as those of the decay phase of the flare, we may have Case D, or possibly a time lag due to turbulent advection.

The result of this technique is shown in Figure 1, for the flare of November 14, 1980, and the scattered power from 70.5 km. The plot of upper left shows a close fit to a line, but not of unit slope. The plot of upper right shows a fairly close fit to a line of slope 1. We may conclude $q = BN$, and more: note that the intercept of this line with the $\log (q_x/q_o) = 0$ line implies that when $q_x = q_o$, $\log (q_x) = 0.3$. Thus we may estimate $q_o = 0.5$ cm^{-3} s^{-1}. The lower plot shows the log scattered power and the estimate of q_x based on the satellite data. The coincidence of the peaks of these curves validates the chemical equilibrium hypothesis, and demonstrates that there is no lag due to turbulent advection.

COMBINED RESULTS FOR SEVERAL FLARES

Figure 2 shows the type of power enhancement found for each altitude for each of seven flare events, arranged in order of decreasing solar zenith angle. The symbol E represents extremely large enhancements (some as much as 30 dB) which cannot be accounted for by this model. Also, note that the altitudes showing no response seem to proliferate downward with increasing solar zenith angle. This is not what Chapman theory predicts for ionization, and so possibly indicates a variability in existence of turbulent layers. Some events, particularly at high zenith angles, show delays (Case D), with delay increasing with decreasing altitude. Note, however, that a delay may be either a chemical or turbulent mixing effect.

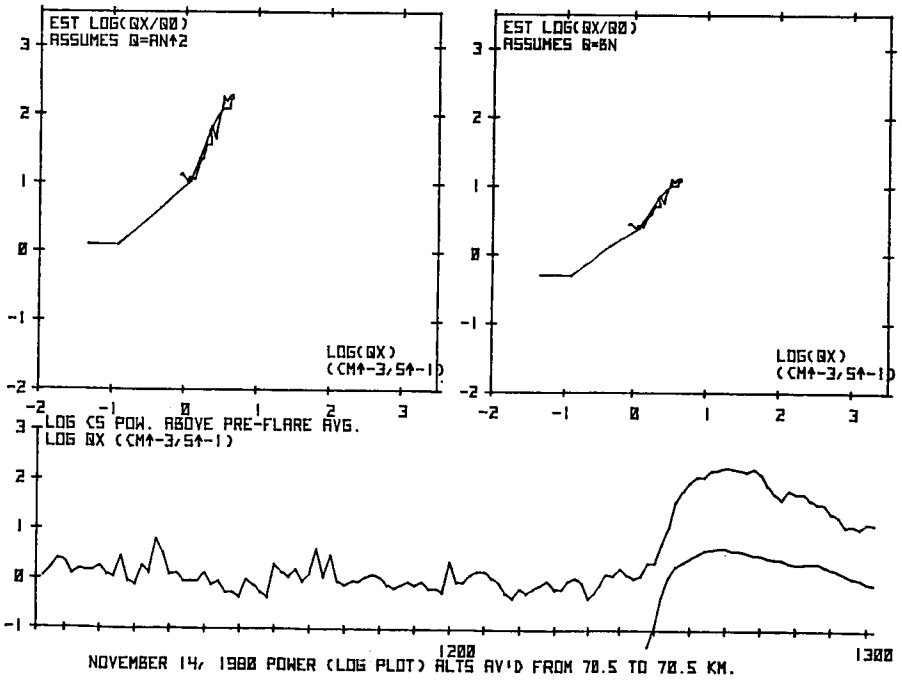

Figure 1. Flare-time scattered power enhancement and estimated electron production rate q_x due to flare X-rays at 70.5 km for the November 14, 1980 event.

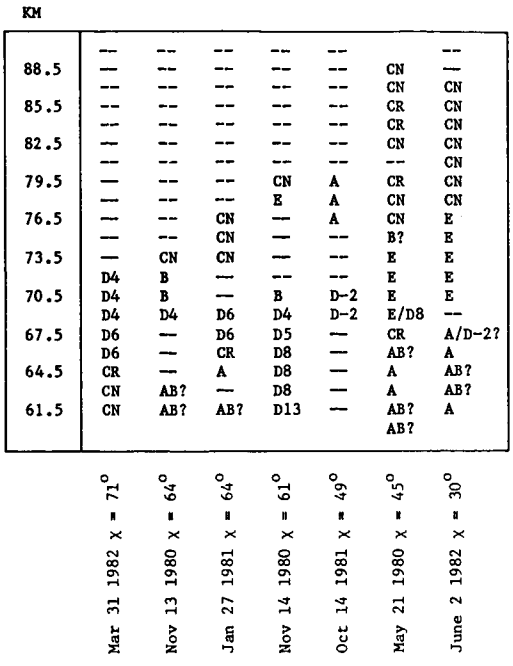

Figure 2. Types of response at each mesospheric altitude for each flare: A) $q = \alpha N^2$. B) $q = \beta N$. AB?) Probably A or B, but plots are ambiguous. D#) Delayed effect, with peak power following q by # minutes. E) Extreme response, power increase greater than cases A or B. CN) Coincident flare-time power response, but unable to fit to A or B model due to comparable nonflare fluctuations in power at that altitude. CR) Coincident response well above nonflare base power, but unable to fit to A or B models due to large fluctuations on the order of the one minute sample time. --) no detectable response.

Figure 3 shows estimates of q_o made by this technique. When the interpretation was unclear between Case A and Case B, but equilibrium seems to hold, a dashed horizontal line indicates the range of possible q_o estimates. Note that the estimates for q_o fall into two clusters, corresponding to small and large zenith angles. Also, the values of q_o for large zenith angle are smaller, as expected. Also, q_o generally increases with altitude for a given flare effect, also as expected. We may conclude that the estimate of q_o has some degree of reliability, although its absolute accuracy is not estimated here.

DISCUSSION AND CONCLUSION

By using models for the uncertain links between the causal X-ray emissions and the coherent-scatter power enhancements, we have gained insights into features which are not otherwise clear. Often one model fits the data better than others, and so we are able to choose between some features of ion-chemical schemes. When no existing model fits the data, as with the extreme power enhancements shown in Figure 3, it is unclear which part of the analysis should be modified: an extreme enhancement may be due to an unknown ion-chemical scheme, or may be due instead to some unknown condition which allows P to increase faster than N^2. This suggests further research.

C-5

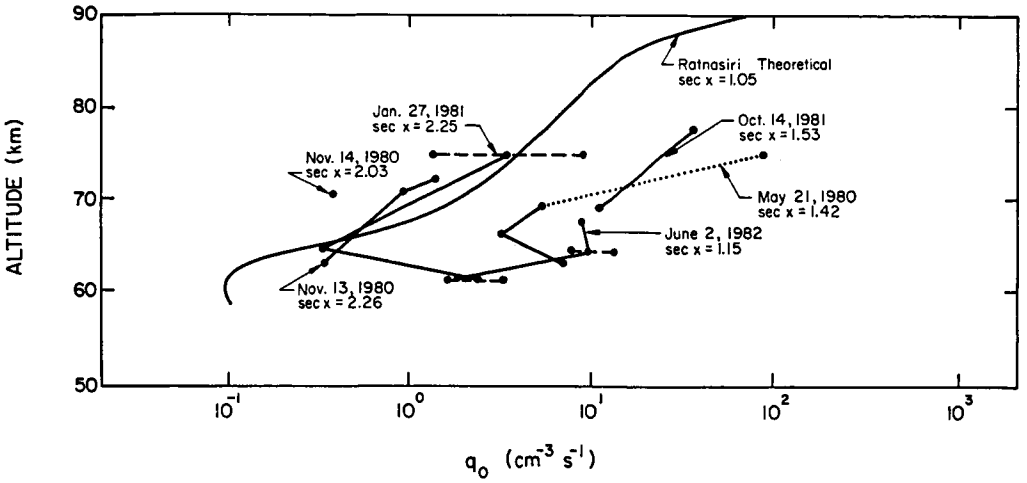

Figure 3. Estimates of q_o made by finding intercept of log (q_x) vs log (q_x/q_o) plots with line log (q_x) $\equiv$ 0 for each altitude and flare event which shows type A ($q_x \equiv \alpha N^2$) or type B ($q_x = \beta N$) response. Horizontal dashed lines represent the span between the type A estimate at q_o and type B estimate at q_o at altitudes where the choice between type A and type B is ambiguous. The estimate of q_o by RATNASIRI and SECHRIST (1975) is reproduced for comparison.

Only altitudes with steady turbulent layers produce useful data, so altitude gaps are inevitable. However, the coherent-scatter radar technique compares favorably with earlier methods of observing changes in N during solar flare, such as partial reflection and wave interaction. The temporal and spatial resolution are excellent for the coherent-scatter technique, and the relative changes in N may be measured accurately.

ACKNOWLEDGMENT

The work described in this paper was supported in part by the National Aeronautics and Space Administration under grant NSG 7506.

REFERENCES

Banks, P. M. and G. Kockarts (1973), Aeronomy, Part A, Academic Press, New York.

Donnelly, R. F. (1977), Solar X-ray measurements from SMS-1, SMS-2, and GOES-1 information for data users, NOAA Technical Memorandum ERL SEL-48.

Miller, K. L., S. A. Bowhill, K. P. Gibbs and I. D. Countryman (1978), First measurements of mesospheric vertical velocities by VHF radar at temperate latitudes, Geophys. Res. Lett., 5, 939-942.

Mitra, A. P. (1974), Ionospheric effects of solar flares, Reidel Publishing Co., Dordrecht-Holland.

Parker, J. W. and S. A. Bowhill (1984), Observations of solar-flare ionization in the mesosphere using coherent-scatter radar, Adv. Space Res., 4, 171-174.

Ratnasiri, P. A. J., and C. F. Sechrist Jr. (1975), An investigation of the solar zenith angle variation of D-region ionization, Aeron. Rep., 67, Elec. Eng. Dep., Univ. Il., Urbana, Il.

Rottger, J. (1983), Origin of refractive index fluctuations in the mesosphere as opposed to the stratosphere and troposphere, Handbook for MAP, Vol. 9, SCOSTEP Secretariat, Dep. Elec. Computer Eng., Univ. IL., Urbana-Champaign, 143-144.

Rowe, J. N., A. J. Ferraro, H. S. Lee, R. W. Kreplin, and A. P. Mitra (1970), Observations of electron density during a solar flare, J. Atmosph. Terr. Phys., 32, 1609-1614.

Thomas, L., P. M. Gondhalekar, and M. R. Bowman (1973), The influence of negative-ion changes in the D-region during sudden ionospheric disturbances, J. Atmosph. Terr. Phys., 35, 385-395.

U. S. Standard Atmosphere, 1976, NOAA, NASA, USAF, U. S. Government Printing Office, Washington.